Chalcogenide Letters Vol. 9, No. 1, January 2012, p. 27 - 40

EFFECT OF PH ON THE PHYSICAL PROPERTIES OF CdS THIN FILMS DEPOSITED BY CBD

A. KARIPER[a], E. GÜNERI[a], F. GÖDE[b], C. GÜMÜŞ[c*]
[a]*Department of Primary Education, University of Erciyes, 38039 Kayseri, Turkey*
[b]*Physics Department, University of Mehmet Akif Ersoy, 15030 Burdur, Turkey*
[c]*Physics Department, University of Çukurova, 01330 Adana, Turkey*

CdS thin films with different pH values changing from 9 to 12 were deposited on glass substrates using chemical bath deposition technique (CBD). The effect of pH on the structural, optical and electrical properties of CdS thin films is investigated. X-ray diffraction, Ultraviolet-visible absorption spectroscopy, Scanning electron microscopy, Energy dispersive X-ray analysis, and Raman spectroscopy were used to characterize the thin films. X-ray diffraction data reveal growth of the cubic phase with preferential orientation along (*1 1 1*) direction. Raman peaks appearing at 296 cm^{-1} and 593 cm^{-1} for all samples were attributed to 1*LO* and 2*LO* phonons of CdS, and they shifted to the blue region with increase in pH values. The band gap of the films increased from 2.29 to 2.40 eV with increasing pH values. Resistivity, carrier density and mobility of the films were determined using Hall effect measurements. After all investigations, it was concluded that the pH value of 11 is suitable for producing CdS thin films by chemical bath deposition technique. The formed film was transparent, uniform and with good adherence to the substrate. These results indicate that films obtained at pH 11 by CBD are good candidates for applications in different optoelectronic devices.

(Recieved December 7, 2011; Accepted January 13, 2012)

Keywords: CdS; Thin films; Chemical bath deposition; pH effect; Raman scattering

1. Introduction

Thin films of II–VI semiconductors (e.g. CdS, ZnS, CdSe, ZnSe) are important for their applications in solid-state solar cells, optical coatings, optoelectronic devices, and light emitting diodes [1]. CdS has a band gap of 2.242 eV and is the most popularly employed heterojunction partner to p-CdTe due to its similar chemical properties [2]. Control of the CdS/CdTe interfacial chemistry is critical in achieving high solar conversion efficiencies.

Several techniques like thermal evaporation [3], RF sputtering [4], hydrothermal method [5], metalorganic chemical vapor deposition [6], sol-gel route [7], chemical bath deposition [8] and spray pyrolysis [9] are widely used for the deposition of thin films. Among these various techniques, chemical bath deposition (CBD) has been recognized as an important route for the manufacture of these materials, since it is a fast, simple and low cost method that results in good quality films that can compete with films obtained by other more sophisticated methods.

Almost no study on how physical properties of CdS films, the authors aim in this work is to investigate the effect of pH on the structural, optical and electrical properties of CdS films. The present article also deals with the deposition of CdS thin films with varied pH and characterization of the deposited films by X-ray diffraction, Raman scattering, scanning electron microscopy, optical absorption spectra and Hall effect measurement.

*Corresponding author: cgumus@cu.edu.tr

2. Experimental details

The CdS films were prepared using aqueous solutions of 10 ml of $Cd(NO_3)_2 \cdot 4H_2O$ (cadmium nitrate) 0.1 M; 10 ml of CH_3CSNH_2 (thioacetamide) 0.1 M; and NH_4OH (ammonium hidroxide). Films were grown on 76 x 26 x 1 mm^3 glass substrates. The film deposition was carried out with the same bath composition with different pH values. In order to adjust pH 9, 10, 11 and 12 of the chemical bath under the control of a pH meter, 100 µl, 200 µl, 2000 µl, 4000 µl of NH_4OH were added to the chemical bath, respectively. The deposition time was 3 h in each case while the whole deposition was carried out at 70 °C. After the depositions, the films were cleaned by flushing with deionized water, and then dried by keeping the samples in open atmosphere at room temperature. The resulting thin films have a yellow color.

The structure, phase purity and microstructural parameters of the films were investigated by using a Rigaku RadB X-ray diffractometer with Cu-Kα_1 line ($\lambda = 1.5405$ Å) in 2θ ranging from 10 to 65° at a speed of 3° / min, with a step size of 0.02°. The Raman spectroscopy was performed at room temperature using a Raman spectrometer (Bruker Senterra) with a 532 nm (20 mW) Ne laser line as an excitation source. Picture of surface morphology and elemental composition of CdS thin films were determined by using computer controlled digital scanning electron microscope (SEM, EVO40-LEO) attached to the EDX system. Resistivity, Hall mobility, and carrier concentration of the films were evaluated by Hall effect measurements at room temperature in a Van der Pauw four-point probe configuration, using indium contacts, in an automated Hall effect system (HS-3000 Manual Ver 3.5). In order to get optical characterization of all deposited films, absorbance and transmission spectra measurements were taken at room temperature by Perkin Elmer UV/vis Lambda 2S spectrophotometer in the wavelength range of 350–1100 nm using a non-coated glass as the reference beam. Thicknesses of the samples were determined by weight difference method [10]. The density of the CdS is taken 4.82 g/cm^3 in bulk form. Fig. 1 shows the variation of the thickness for the CdS films as a function of pH value of the reaction mixture for a constant dipping time of 3 h. It was clearly seen from figure that the thickness of the deposited films decreased from 563 to 111 nm with increase in pH values. The bath temperature can be effectively used to control the rate of CdS formation.

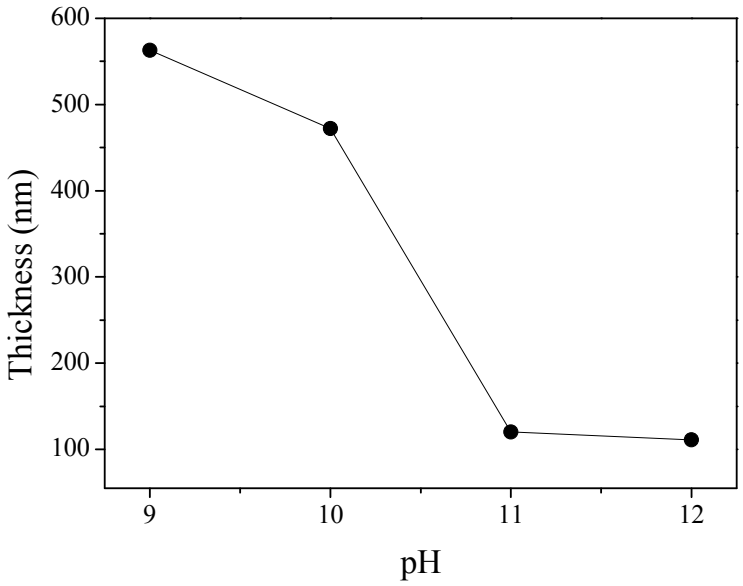

Fig. 1: Thickness of the CdS thin films deposited at different pH values for a constant dipping time of 3 h.

3. Results and discussion

3.1. Structural properties

Fig. 2 shows the XRD spectrum for the CdS thin films deposited at different pH values. The films prepared at pH values of 9, 10 and 11 exhibited cubic structure, specifically (*1 1 1*) and (*2 2 0*) planes [11]. The film deposited at pH value 12 did not show any peak, indicating the amorphous character of the deposited film. The diffraction peak observed close to 2θ~26.638 (for pH = 9, 10 and 11) becomes much broader with increasing the pH values and disappears for the pH value of 12. Similar pH effect was observed in Ref. [12] in which ZnS thin films were grown by chemical bath deposition. As the pH of chemical bath increased, the diffraction peak intensity considering (*1 1 1*) plane decreased in Fig. 2, indicating decreased crystallinity. It can be seen that the crystal structure of the films was affected strongly by the pH values of the chemical bath.

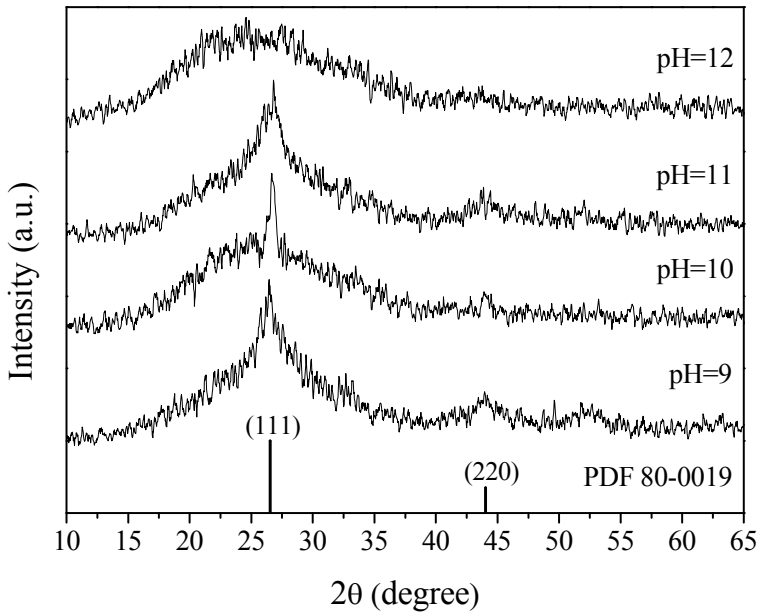

Fig. 2: X-ray diffraction patterns of the CdS thin films deposited on glass substrates at different pH of chemical bath.

The lattice constants (a) for (*1 1 1*) plane of CdS films with varied pH values from 9 to 11 are obtained from the X-ray analysis using the following relationship for cubic crystal [13]:

$$a = d\sqrt{h^2 + k^2 + l^2} \tag{1}$$

For the CdS thin films deposited at different pH values of chemical bath, the observed diffraction angle 2θ, interplanar spacing (d), miller indices (*h k l*) and calculated lattice parameter (a) compared with the standard values are listed in Table 1. It can be seen from Table 1 that lattice constant (a) decreased from 5.844 Å to 5.719 Å, while the diffraction angle 2θ shifted to higher angles with increasing pH values from 9 to 11.

Table 1: Comparison of diffraction angle (2θ), the interplanar spacing (d), lattice constant (a) and miller indice (h k l) between observed and standard values of the CdS films.

H	$2\theta_{Obs.}$ (°)	$2\theta_{PDF}$ (°)	$d_{Obs.}$ (Å)	d_{PDF} (Å)	$a_{Cal.}$ (Å)	a_{PDF} (Å)	(*hkl*)
9	26.389	26.547	3.374	3.355	5.844	5.811	(111)
10	26.638	26.547	3.345	3.355	5.794	5.811	(111)
11	26.982	26.547	3.302	3.355	5.719	5.811	(111)

Table 2: Compositional analysis of the CdS thin films deposited at different pH of the chemical bath.

pH	Elements	Atomic (%)	Atomic ratio (Cd/S)
9	Cd	22.39	1.05
	S	21.20	
10	Cd	14.63	1.05
	S	13.91	
11	Cd	5.80	1.18
	S	4.91	
12	Cd	2.90	0.98
	S	2.94	

Table 3: The first and second order LO Raman phonons of polycrystalline CdS thin films with varied pH of the chemical bath.

pH	Observed Raman shift (cm^{-1})	
	$1LO$	$2LO$
9	296	593
10	298	597
11	304	600

The grain sizes (D) were calculated using the Scherrer's formula [14] from the full-width at half-maximum (FWHM):

$$D = \frac{0.9\lambda}{\beta cos\theta} \tag{2}$$

where β is the full width at half maximum, λ is the wavelength of X-ray used, θ is the Bragg's angle. As shown in Fig. 3, the grain size calculated considering the (*1 1 1*) plane was decreased from 26 nm to 19 nm with increase in pH values.

A dislocation is an imperfection in a crystal associated with the misregistry of the lattice in one part of the crystal with that in another part. Unlike vacancies and intersitial atoms, dislocations are not equilibrium imperfections, i.e., thermodynamic considerations are insufficient to account for their existence in the observed densities. Infact, the growth mechanism involving a dislocation is a matter of importance in Ref. [15]. The dislocation density (δ), defined as the length of dislocation lines per unit volume of the crystal, was evaluated from the below formula [16]:

$$\delta = \frac{1}{D^2} \tag{3}$$

As the pH values of the chemical bath increases, the dislocation density decreases (Fig. 3). The origin of strain (ε) is related to the lattice misfit, which in turn depends upon the deposition conditions. The strain was calculated using the relation:

$$\varepsilon = \frac{\beta \cos\theta}{4} \tag{4}$$

Fig. 3 also shows that while the pH values of chemical bath increases, strain decreases. This is due to the passive recrystallization process in the polycrystalline thin films and due to the movement of intersitial cadmium atoms from inside the crystallites to the grain boundaries which dissipate, and lead to a reduction in the lattice imperfection.

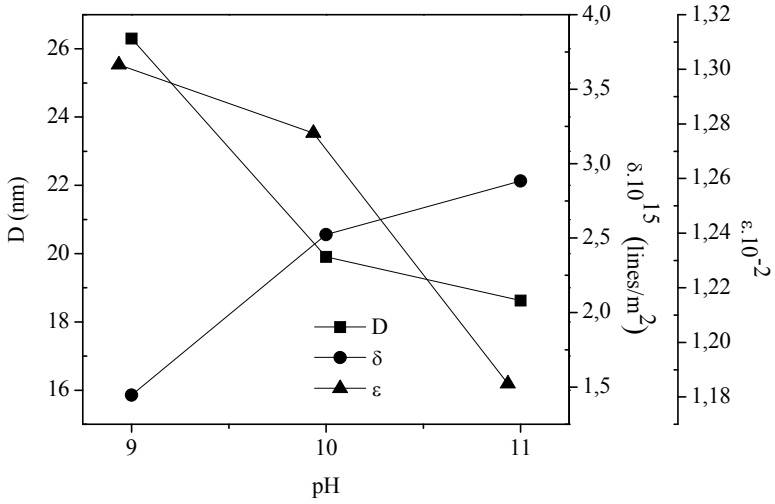

Fig. 3: Variation of the grain size (D), the dislocation density (δ) and the strain (ε) with the pH of the chemical bath.

Quantitative analysis of the film was carried out using the EDX technique to study stoichiometry of the film. EDX analysis results show that Cd and S elements in the starting solution present in the solid film. The detailed results of the EDX analysis are listed in Table 2. It shows that the films deposited at pH 11 were slightly cadmium rich while the films deposited at pH 12 were sulphur rich. It was significant to note that films deposited at both pH 9 and pH 10 is nearly stoichiometric.

3.2. Morphological studies

The surface morphology of the deposited films was investigated by scanning electron microscopy (SEM). Fig. 4 shows the micrographs of CdS thin films deposited at different pH values. From Fig. 4a, The author conclude that CdS film deposited at pH 9 is consists of clusters of up to 22 nm, but clearly these clusters were formed due to a coalescence of small grains of

about 2.5 nm. Fig. 4b shows the SEM micrograph of the CdS film deposited at pH 10, where the film has clusters of up to 15 nm and the clusters consists of coalescence of small grains of about 1.7 nm. Fig. 4c depicts the SEM image of the CdS film deposited at pH 11, which reveals a homogeneous and compact nanocrystalline structure composed of spherically shaped and well defined grains of 3.3 nm. Fig. 4d reveals that although some naked areas exist, deposited CdS film is homogeneous and distributed on the basal plane on the edge plane surface of the substrate. These results show that when the pH value of the chemical bath increases, the number of clusters decreases. This means that the surface morphology of the films is strongly influenced by the pH of chemical bath.

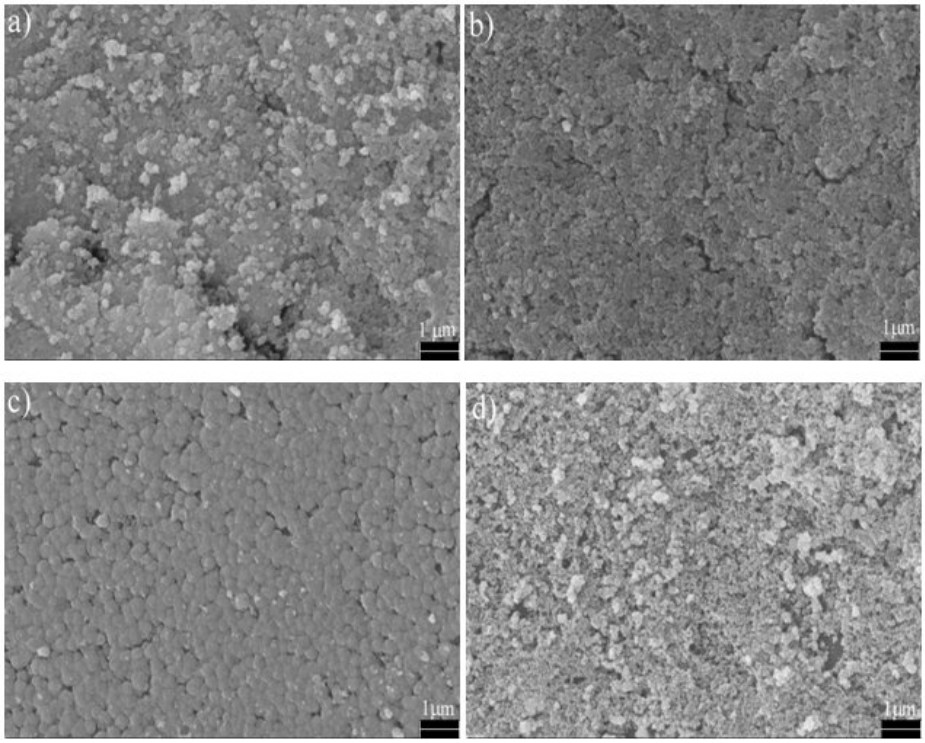

Fig. 4: SEM micrograph of the CdS thin films deposited on glass substrate at different pH values, (a): 9, (b): 10, (c): 11 and (d): 12.

3.3 Raman studies

Raman spectroscopy has been recognized as a very sensitive tool for characterizing crystalline structures of CdS, including lattice defect, grain boundries, stacking faults, twins or a combination thereof. The 1*LO* and 2*LO* phonon frequencies of the bulk CdS crystal were reported previously [17] at 305 and 604 cm^{-1}, respectively.

As shown in Fig. 5, the Raman spectra of the prepared CdS films with varied pH values exhibit two different specific bands. These two peaks identified at 296 cm^{-1} and 593 cm^{-1} for the prepared CdS films indicate the first and second order longitudinal optical phonon (*LO*) modes of the CdS crystal. The result is similar to that of the bulk crystal [17] and consistent with previous studies of CdS thin films [18,21]. Table 3 also shows the first and second order LO Raman phonons of polycrystalline CdS thin films with different pH values. As seen from this table that the first and second order Raman peaks observed at 296 cm^{-1} and 593 cm^{-1} shifted in to the blue region. This slight shift to the lower wavelengths of the thin films might be attributed to the effect caused by the grain size [22,23] or the effect of the surface phonon mode [24]. It can be seen from Fig. 5 that the Raman peaks intensities of the films decreased as the pH values increased from 9 to 11. This reduction observed on Raman phonons of the films is also consistent with the change of XRD patterns shown in Fig. 2, and does not reported before.

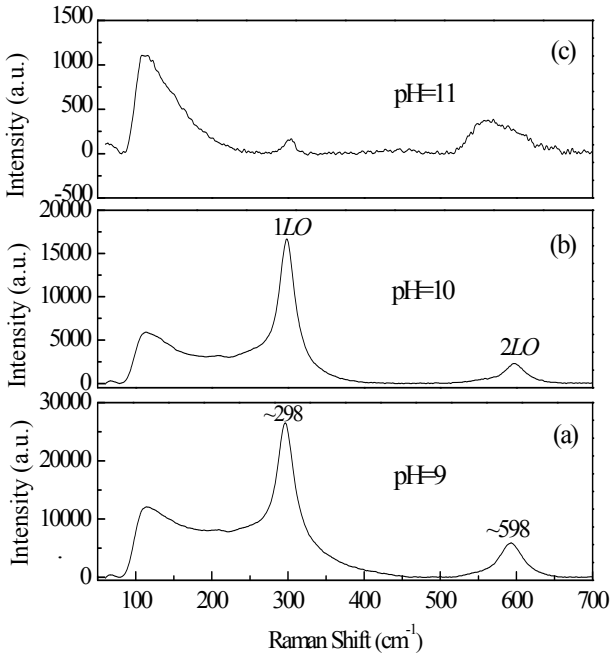

Fig. 5: Raman spectra of the CdS thin films with different pH values, (a): 9, (b): 10 and (c):11.

3.4. Optical Properties

The transmittance of the CdS thin film is expected to depend on three factors: (1) oxygen deficiency, (2) surface roughness (surface scattering reduces the transmission, which in turn depends on the grain size and shape) and (3) impurity centers.

The transmission of the films was measured with a blank glass as reference. The transmission spectra of the CdS thin films deposited at different pH values of the chemical bath are shown in Fig. 6. It can be seen that transmission improved slightly with the increase in pH values. All deposited films exhibited transmittance between 40% and 85% in the visible region, and showed the fundamental absorption edge in the range 470–540 nm. As shown in Fig. 7, the reflection spectra of the films decreased with increasing pH values.

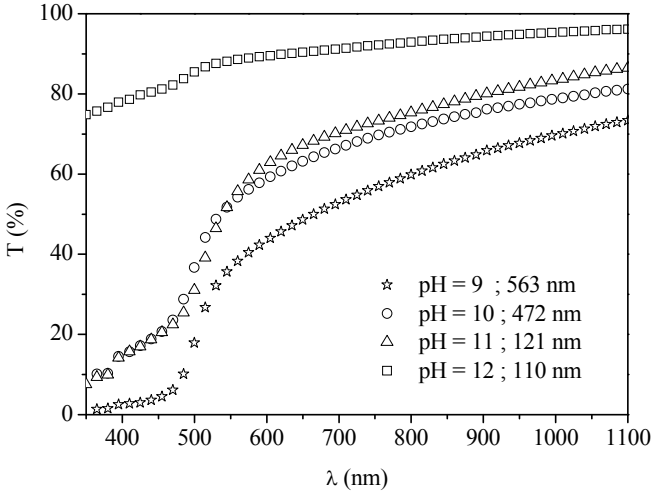

Fig. 6: Optical transmission spectra of the CdS thin films deposited at different pH values.

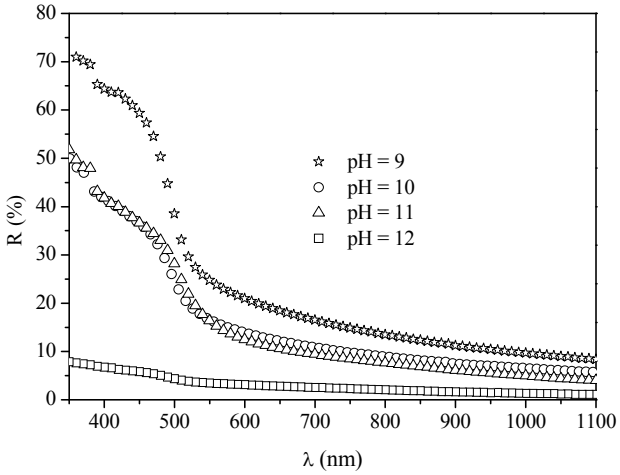

Fig. 7: Optical reflection spectra of the CdS thin films deposited at different pH.

The optical absorption coefficient α was calculated for each film using the following equation [25]:

$$T = (1 - R)^2 \, exp(\alpha t) \tag{5}$$

where T is the transmittance, R is the reflectance and t is the film thickness. The variation of the optical absorption coefficient with wavelength was analyzed to find out the nature of the electronic transition across the optical band gap. The nature of the transition was determined using the relation:

$$\alpha h\nu = A\left(h\nu - E_g\right)^{n} \tag{6}$$

where A is *a* constant, h is the Plank constant, ν is the frequency of photons and n equals to ½ for direct band gap [26]. The band gap E_g can be obtained by extrapolating the straight line of $(\alpha h\nu)^2$ vs. $h\nu$ curve to intercept the horizontal $h\nu$ axis. The direct band gap E_g of all the samples can be obtained as shown in Fig. 8. From this figure, it can be seen that the direct band gap of the samples increased from 2.29 to 2.40 eV with increasing pH values (Table 4). Obtained band gap values closely agree with the previous reported values for the CdS thin films deposited by different techniques such as thermal evaporation [27], chemical bath deposition [19,28] and spray pyrolysis [29].

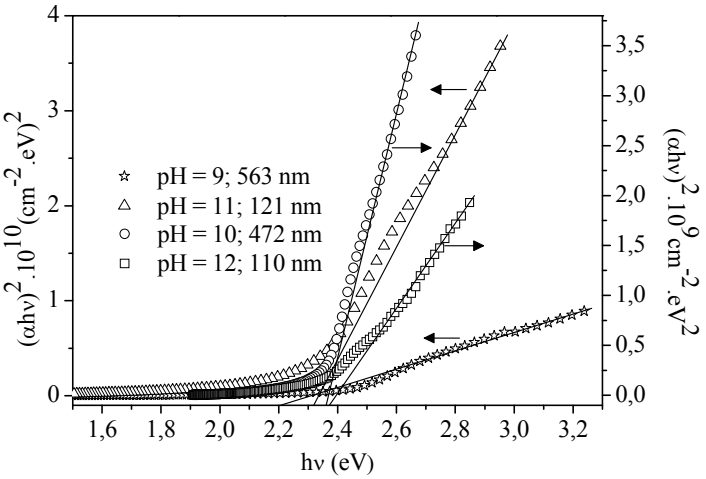

Fig. 8: $(\alpha h\nu)^2$ *vs.* $h\nu$ *curve of the CdS thin films deposited with varied pH values.*

3.5. The refractive index and extinction coefficient of the films

The refractive index plays an important role in the search for optical materials, being a significiant factor in optical commnication and in designing devices for spectral dispersion. Therefore, it is important to determine refractive index of the thin film. Figs. 6 and 7 show the transmittance T and the reflectance R spectra of the films in the UV-visible range. The optical constants the refractive index (n) and extinction coefficient (k) were calculated from T and R spectra of the films. The refractive index and extinction coefficient are expressed as below formulas [30]:

$$k = \frac{\alpha\lambda}{4\pi} \tag{7}$$

$$n = \frac{1+R}{1-R} + \sqrt{\frac{4R}{(1-R)^2} - k^2} \tag{8}$$

The variation of the refractive index of the CdS films with varied pH values is shown in Fig. 9, and the obtained values of it are listed in Table 4. It was seen that at the wavelength of 550 nm, the refractive index of the film decreased from 2.98 to 1.46 with increasing pH from 9 to 12. The decrease in the refractive index is associated with the fundamental band gap absorption. The changes in the refractive index indicate that some interactions take place between photon and electrons in the thin film. It is clearly evident that a peak appeared in the refractive index, which shifts to the higher energies. This shift confirms the increase in the optical band gap. Furthermore, the dependence of extinction coefficient on wavelength is shown in Fig. 10, and its values are also listed in Table 4. It is seen that the extinction coefficient changes in the range 0.021–0.099 at the wavelength of 550 nm. As a result, the values of both n and k are decreased with increasing wavelength.

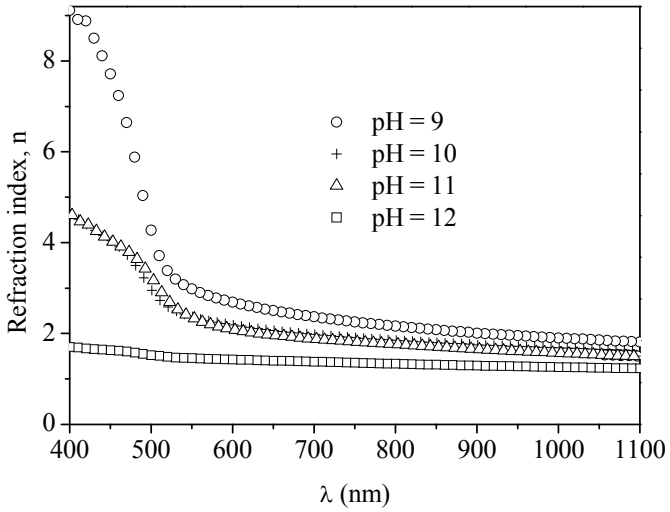

Fig. 9: The dependence of the refractive index (n) *on wavelength* (λ) *as a function of the pH values for the CdS thin films.*

3.6. Dielectric function of the films

It is well known that polarizability of any solid is proportional to its dielectric constant. $\varepsilon^* = \varepsilon_1 + i\varepsilon_2$ characterizes the optical properties of any solid material. The real (ε_1) and imaginary (ε_2) parts of the dielectric constant were determined by the following relations [31]:

$$\varepsilon_1 = n^2 - k^2 = \varepsilon_\infty - \frac{e^2}{4\pi^2 c^2 \varepsilon_0}\frac{N}{m^*}\lambda^2 \tag{9}$$

$$\varepsilon_2 = 2nk = \frac{\varepsilon_\infty \omega_p^2}{8\pi^2 c^3 \tau}\ \lambda^3 \tag{10}$$

where ω_p is the plasma frequency, ε_∞ is the high frequency dielectric constant, e is the electronic charge, N is the free carrier concentration, m^* is the effective mass of free carrier, τ is the optical relaxation time, and c is the velocity of light. The real and imaginary parts of the dielectric constant were calculated by using the n and k values calculated via Eqs. (9) and (10). The dependence of the real part of the dielectric constant on wavelength is shown in Fig. 11. From this figure and Table 4, it can be seen that it decreases from 8.890 to 2.122 at wavelength of 550 nm with increasing pH values, and tends to be constant at higher wavelengths. Besides, variation of the imaginary part of the dielectric constant as a function of wavelength is shown in Fig. 12. From this figure and Table 4, the imaginary part of the dielectric constant changes in the range 0.063–0.469 at wavelength of 550 nm.

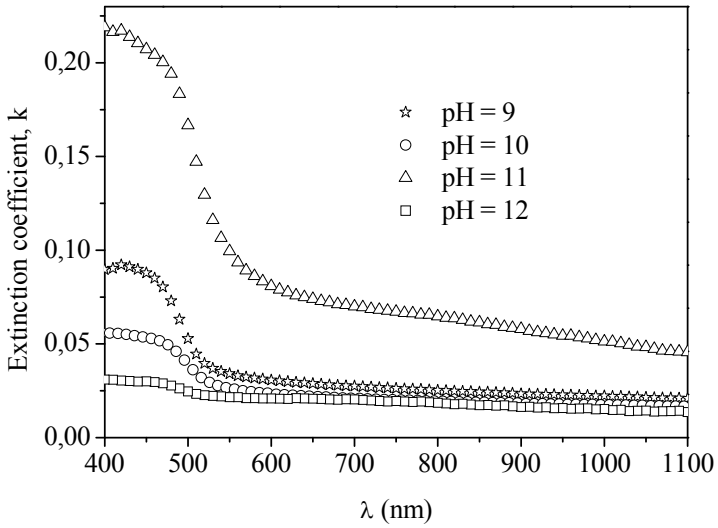

Fig. 10: The dependence of the extinction coefficient (k) on wavelength (λ) as a function of the pH values for the CdS thin films.

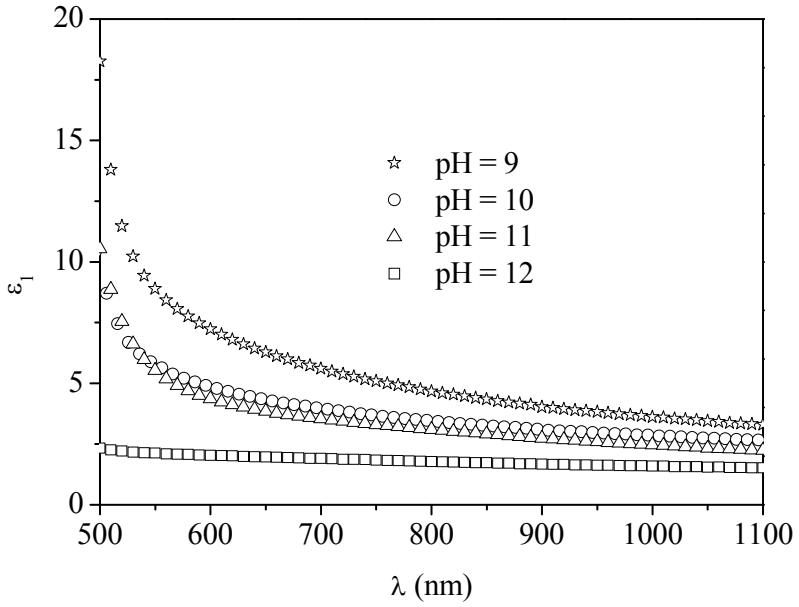

Fig. 11: Variation of the real part (ε_1) of the dielectric constant with wavelength (λ) as a function of the pH values for the CdS thin films.

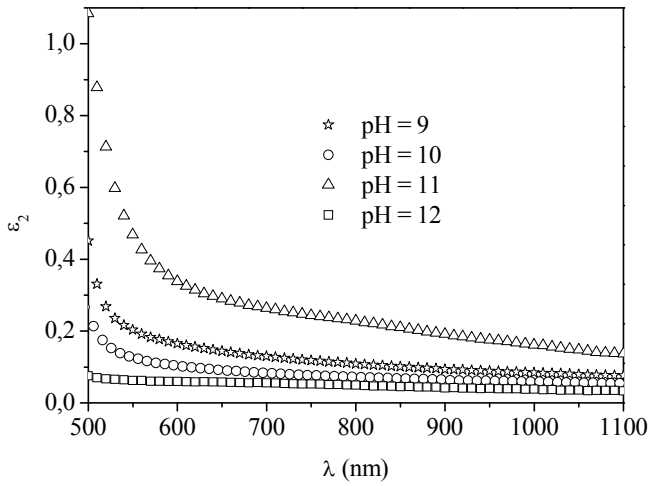

Fig. 12: Variation of the imaginary part (ε_2) *of the dielectric constant with wavelength* (λ) *as a function of the pH values for the CdS thin films.*

Table 4: The optical band gap (E_g)*, the refractive index* (n)*, the extinction coefficient* (k)*, the real* (ε_1) *and imaginary* (ε_2) *parts of dielectric constant with different pH values.*

pH	E_g (eV)	n	k	ε_1	ε_2
9	2.29	2.98	0.034	8.890	0.203
10	2.37	2.38	0.026	5.778	0.126
11	2.33	2.35	0.099	5.534	0.469
12	2.40	1.46	0.021	2.122	0.063

3.7. Electrical Properties

Electrical resistivity, carrier concentration and carrier mobility of the CdS films were measured using van der Pauw geometry and Hall effect measurement at room temperature using indium ohmic contacts. Hall resistivity, the mobility and the carrier concentration of the CdS films with increasing pH values are shown in Fig. 13. The resistivity ρ is proportional to the reciprocal of product of the free carrier concentration N and the mobility μ as is shown the following relation [32]:

$$\rho = \frac{1}{Ne\mu} \tag{11}$$

The resistivity of the CdS films was dominated by the free carrier concentration and mobility. The low mobility and carrier concentration may result in high resistivity. It is seen in Fig. 13 that the resistivity of the CdS films decreased from $4.72\text{x}10^5$ to $4.80\text{x}10^4$ Ω·cm with increase in pH values, and these values are lower than the literature values [33,34] in which the CdS thin films were prepared by spray pyrolysis technique. Furthermore, decreasing resistivity with the increasing pH values may be attributed to both size and dimension of the confinement [35]. The lowest resistivity value calculated as $4.80\text{x}10^4$ Ω·cm at pH 11 in the authors work is very suitable for solar cells. Moreover, it was clearly seen from Fig. 13 that the CdS film with pH 11 has the best conductivity value. From this figure, the mobility of the deposited films increased

from 29.46 to 50.70 $cm^2\ V^{-1}\ s^{-1}$ with increasing pH values and these values are in agreement with that of chemical bath deposited CdS films [36] and and these results are lower than what other researchers have observed earlier for the CdS thin films by using a rapid and simple solvothermal route (62.83 $cm^2\ V^{-1}\ s^{-1}$) [37]. Moreover, in Fig. 13, the carrier concentration of the films increased from $2.60x10^{11}$ to $4.41x10^{12}$ cm^{-3} with incrase in pH and the values are in agreement with Ref. [36], but remarkably lower than that of Cd-rich films by CBD [38] than the previous works [29,37].

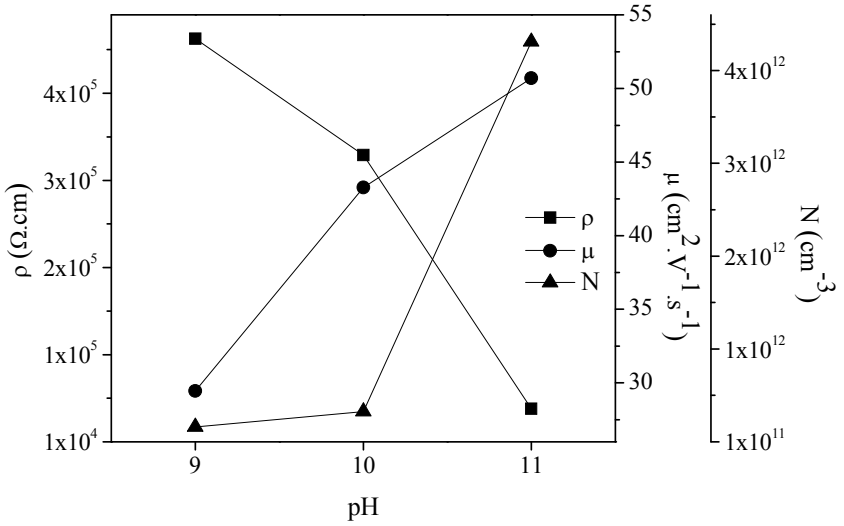

Fig. 13: Variation of the Hall resistivity (ρ)*, the Hall mobility* (μ) *and the carrier concentration* (N) *with pH values for the CdS thin films.*

4. Conclusions

Polycrystalline, nearly stoichiometric CdS thin films with different pH values were prepared on glass substrates by chemical bath deposition. The structural, optical and electrical properties of the CdS films were found to vary with the pH value of the chemical bath. XRD analysis confirmed the crystalline formation of cubic CdS films. The grain size of the films decreased with increasing pH values from 9 to 11. Raman peaks appearing at 296 cm^{-1} and 593 cm^{-1} for all samples were attributed to 1*LO* and 2*LO* phonons of the CdS. These peaks shift to the blue region with an increase in pH values. The formation of the CdS thin films is also confirmed by Raman analysis. It should be noted that the effect of pH on the crystal structure of the CdS films using Raman spectroscopy is reported for the first time in this work. The resistivity of the CdS thin films decreased from $4.72x10^5$ to $4.80x10^4$ Ω·cm with increasing pH values. The band gap of the samples increased from 2.29 to 2.40 eV with increasing pH values of the chemical bath from 9 to 12. These results indicate that films obtained at pH 11 with wide band gap, low resistivity, high mobility and high carrier concentration by CBD are good candidates to be applied in different optoelectronic devices. Moreower, the efficiencies of p-CdTe/n-CdS thin film solar cells can be increased by adjusting the chemical bath to pH 11.

References

[1] Han J, Spanheimer C, Haindl G, Fu G, Krishnakumar V, Schaffner J, Fan C, Zhao K, Klein A, Jaegermann W. Sol Energy Mater Sol Cells; **95**, 816 (2011).
[2] Mendoza-Pérez R, Sastre-Hernández J, Contreras-Puente G, Vigil-Galán O. Sol Energy Mater Sol Cells; **93**, 79 (2009).

[3] O. Toma, R. Pascu, M. Dinescu, C. Besleaga, T.L. Mitran, N. Scarisoreanu, S. Antohe, Chalcogenide Letters, **8**(9), 541 (2011).
[4] Assali KE, Boustani M, Khira A, Bekkay T, Outzourhit A, Ameziane EL, Bernede JC, Pouzet J Phys Status Solidi (a);**178,** 701 (2000).
[5] Sanjeev K, Ramesh Chandra. J. Optoelectron. Adv. Mater. **13**,(8), 952 (2011).
[6] Uda H, Yonezawa H, Ohtsubo Y, Kosaka M, Sonomura H. Sol Energy Mater Sol Cells; **75,** 219 (2003).
[7] Boev VI, Soloviev A, Rodríguez-González B, Silva CJR, Gomes MJM. Mater Lett **60**, 3793 (2006).
[8] G. Bakiyaraj, N. Gopalakrishnan and R. Dhanasekaran, Chalcogenide Letters, **8**(7), 419 (2011).
[9] E. Elangovan, M. P. Singh, M. S. Dharmaprakash, K. Ramamurthi, J. Optoelectron. Adv. Mater., **6**(1), 197 (2004).
[10] Chopra KL. Thin Film Phenomena. New York: McGraw Hill Book Co; 1969.
[11] PDF Data File No. 80-0019.
[12] Nasr TB, Kamoun N, Kanzari M, Bennaceur R. Thin Solid Films **500,** 4 (2006)
[13] Pejova B, Tanuevski A, Grozdanov I. J Solid State Chem; **177**, 4785 2004
[14] E. Guneri, F. Gode, C. Ulutas, F. Kirmizigul, G. Altindemir, C. Gumus, Chalcogenide Letters **7**(12), 685 (2010).
[15] De CK, Mishra NK. Indian J Phys **A71**, 530. 1997
[16] Williamson GB, Smallman RC. Phil Mag; **1,** 34 (1956).
[17] Klein MV, Porto SPS. Phys Rev Lett; **22,** 782 (1969).
[18] Jana A, Bhattacharya C, Datta J. Electrochim Acta 2010;55:6553.
[19] S. J. Castillo, A. Apolinar-Iribe, D. Berman-Mendoza, R. Ramirez-Bon, Chalcogenide Letters **8**(10), 631 (2011).
[20] Lee J. Thin Solid Films; **451–452**, 170 (2004).
[21] Wan L, Bai Z, Hou Z, Wang D, Sun H, Xiong L. Thin Solid Films; **518,** 6858 (2010).
[22] Briggs RJ, Ramdas AK. Phys Rev B 1976;135518.
[23] Jerominek H, Pigeon M, Patela S, Jakubczk Z, Delisle C, R. Tremblay R. J Appl Phys 63957, 1988
[24] Ren T, Lei Z, Luan G, Jia G, Zhang J, Yu R, Li C. Thin Solid Films; **513,** 99 (2006).
[25] Pankove J. Optical Processes inSemiconductors. New York; Dover Publications; 1971.
[26] Singh M, Mehta BR, Varandani D, Singh VN. J Appl Phys;**106**, 053709-1 (2009).
[27] N. M. Shah, J. R. Ray, M. S. Desai, C. J. Panchal, J. Optoelectron. Adv. Mater., **12**(10), 2052 (2010).
[28] Khallaf H, Chai G, Lupan O, Chow L, Park S, Schulte A. Appl Surf Sci; **255,** 4129 (2009).
[29] Kose S, Atay F, Bilgin V, Akyuz I, Ketenci E. Appl Surf Sci; **256,** 4299 (2010).
[30] F. Göde, C. Gümüş, M. Zor, J. Optoelectron. Adv. Mater., **9**(7), 2186 (2007).
[31] Wakad MM, Shokr EKh, Mohammed SH. J Non-Cryst Solids **265,** 157 (2000).
[32] Takada S. J Appl Phys **73**, 4739 (1993).
[33] Atay F, Bilgin V, Akyuz I, Kose S. Mat Sci Semicon Proc; **6,** 197 (2003).
[34] Orlianges JC, Champeaux C, Dutheil P, Catherinot A, Mejean TM. Thin Solid Films 2011;doi:10.1016/j.tsf.2010.12.139.
[35] Marquardt P, Nimtz G, Muhlschlegel B. Solid State Commun; **65**, 539 (1988).
[36] Liu F, Lai Y, Liu J, Wang B, Kuang S, Zhang Z, Li J, Liu Y. J Alloys Compd **493,** 305 (2010).
[37] Yan S, Sun L, Qu P, Huang N, Song Y, Xiao Z. J Solid State Chem **182,** 2941 (2009).